

Droplet bistability and its application to droplet control

Beomjoon Lee · Jung Yul Yoo

Received: 6 April 2011 / Accepted: 11 June 2011 / Published online: 22 June 2011
© Springer-Verlag 2011

Abstract Novel methods for controlling droplets precisely in the microchannels are presented, which employ microfluidic bifurcation channels with outlet restrictions based on droplet bistability, utilizing the Laplace pressure caused by interfacial tension that arises when a droplet encounters a narrow restriction. The bistable geometry possesses two symmetric branches and restrictions that operate as capillary valves allowing a droplet to be trapped in front of a restriction and released through it when the next droplet arrives at the other restriction. This trap-and-release occurs repeatedly and regularly by the succeeding droplets. Furthermore, a critical flow rate is found to exist, which is necessary for achieving droplet bistability. This occurs only when the apparent Laplace pressure surpasses the pressure drop across the droplet. By adopting a simplified hydrodynamic resistance model, the droplet bistable mechanism is clearly explained, and droplet bistability is shown to enable the simple and precise control of droplets at a bifurcation channel. Thus, precise droplet traffic control is achieved at a bifurcation channel connected with a single inlet channel and two outlet channels using an appropriate channel design that induces droplet bistability. In particular, droplets are distributed at a junction in a manner of perfect alternation or perfect switching between

the two outlet channels. This article proposes that bistable components can be used as elaborately embedded droplet traffic signals for red light (trap), green light (release), and turn light (switching) in complex microfluidic devices, where droplets provide both the chemical or biological materials and the processing signal.

Keywords Droplet · Bistability · Microfluidic logic · Droplet traffic control

1 Introduction

Droplet-based lab-on-a-chip devices in which a segmented liquid flow precisely performs various tasks in a microchannel have received increasing attention in terms of micro total analysis systems (μ TAS). Since droplets act like independent picoliter reactors, droplet-based microfluidics desirably consume small sample amounts. Furthermore, droplets remain free of contamination from the outer environment, do not evaporate because of the presence of a continuous phase, and rapidly mix without dispersion (Shim et al. 2007). Because of such advantages, droplet-based microfluidics have been applied to protein crystallization (Shim et al. 2007), cell encapsulation (Shintaku et al. 2007; Chabert and Viovy 2008), nano particle synthesis (Hung et al. 2006), chemical mixing (Chabert et al. 2005), sol–gel reactions (Chokkalingam et al. 2010), and so forth. In general, lab-on-a-chip devices consist of several serial compartments that perform basic functions such as droplet generation (Thorsen et al. 2001; Nisisako et al. 2002), droplet trap-and-release (Schmitz et al. 2009; Huebner et al. 2009; Bai et al. 2010), droplet path control (Engl et al. 2005; Jousse et al. 2006; Cristobal et al. 2006; Tan et al. 2008; Cybulski and Garstecki 2010),

Electronic supplementary material The online version of this article (doi:10.1007/s10404-011-0834-1) contains supplementary material, which is available to authorized users.

B. Lee
School of Mechanical and Aerospace Engineering,
Seoul National University, Seoul 151-744, Korea

J. Y. Yoo (✉)
Institute of Advanced Machinery and Design,
Seoul National University, Seoul 151-744, Korea
e-mail: jyyoo@snu.ac.kr

and droplet merging (Tan et al. 2007; Niu et al. 2008; Jin et al. 2010). In order to achieve high throughput screening (HTS), integrating multiple serial processes of the device into a single chip in a parallelized manner has been attempted. Such integration requires precise droplet control, especially at the interconnected junctions where the paths of the droplets are determined.

Droplets can be controlled by an active or a passive method. For an active control, lab-on-a-chip devices require external components such as electrical control systems (Wang et al. 2009), pneumatic valves (Lee et al. 2007, 2009), or acoustic waves (Franke et al. 2009; Ahmed et al. 2009). These external components complicate the entire system, which limits convenience, robustness, and portability. The on-chip flow control method utilizing embedded non-electrical flow control devices has been widely adopted in order to reduce the complexity of a system (Mosadegh et al. 2010).

Passive methods utilize hydrodynamic forces to control droplets, which are locally varied either by the geometry of the microchannel, or by the surface property. In particular, microfluidic logic fields provide great opportunities to control the fluid flow in microchannels. Although the microfluidic logic operation on bubbles or droplets cannot compete with the ability of the electrical logic circuit, it provides a powerful method to implement a fully functional chemical process onto a microfluidic device (Cybulski and Garstecki 2010). Universal boolean logic (Cheow et al. 2007; Prakash and Gershenfeld 2007), microfluidic timer (Toepke et al. 2007), and droplet-based shift register (Zagnoni and Cooper 2010) have been successfully implemented in multiphase flows, utilizing nonlinear hydrodynamic interactions between bubbles or droplets that flow in microchannels. Meanwhile, Prakash and Gershenfeld (2007) reported bubble bistability by which bubbles can be trapped and released alternatively in symmetric microchannels as a part of microfluidic bubble logic circuit.

Bistability possesses several advantages over other passive methods for droplet control. First, the bistable mechanism does not depend on its operating frequency. Therefore, it is applicable to the time-varying flow condition while most passive methods for droplet traffic control at the bifurcation channel require a well-established flow condition with a narrow band of operating frequencies (Cristobal et al. 2006; Tan et al. 2004). Second, the bistable mechanism is robust because it utilizes a relatively large hydrodynamic force related to the Laplace pressure induced by the deformation of the interface of the fluids. Third, the bistability can switch the direction of the flow in an alternating manner without any external components, providing a simple but powerful method for droplet traffic control. Fourth, the bistability provides cascading and scalability so that function implementation is simple with any

microfluidic device for a serial process (Prakash and Gershenfeld 2007). Moreover, the bistability can be applied to any immiscible liquid because it relies on the hydrodynamic interactions between interfaces. These characteristics are desirable for droplet control at the interconnected junction where complexity of the flow of droplets arises.

Therefore, this study proposes novel methods for droplet control by utilizing droplet bistability in microchannels. We exploit the bistable geometry in microchannels and conduct a quantitative study to uncover flow conditions such as droplet velocity and droplet length for the onset of droplet bistability. Furthermore, we distribute droplets at a junction with elaborately designed interconnections where the droplets perfectly alternated or perfectly switched between the two outlet channels. Then, droplet bistability is shown to enable simple and precise droplet control techniques such as trap-and-release, synchronization, merging, and traffic control.

2 Materials and methods

The microfluidic channel was fabricated using conventional soft-lithography techniques (Xia and Whitesides 1998). The SU-8 2050 (MicroChem) negative photo resist was spin-coated on a silicon wafer and soft baked for 6 min at 65°C and subsequently for 20 min at 95°C. Soft-baked molds were exposed to a near-UV light source with a photomask, post-baked for 1 min at 65°C, and subsequently for 5 min at 95°C, and developed in the SU-8 developer (MicroChem). A mixture of Polydimethylsiloxane (PDMS) base and curing agent (10:1 w/w, DA-184A and DA-184B, Dow Corning) was poured onto the fabricated SU-8 master; it was then cured at 90°C for 1 h. The patterned PDMS mold was carefully peeled off from the silicon substrate and punched for inlet and outlet ports. To fabricate the bottom layer, a 10:1 PDMS mixture was spin-coated on the glass substrate at 500 rpm for 30 s and was cured at 90°C for 1 h. This bottom layer provided a uniform surface condition for fluids and it provided system stability. The patterned layer and bottom layer of the PDMS were irreversibly bonded to each other by an air plasma treatment at 700 mTorr for 150 s. Prior to use, the fabricated PDMS channels were placed in an 80°C oven for 24 h to insure that the hydrophilic surface from the plasma-treated PDMS returns to the hydrophobic surface. We fabricated three different PDMS channels with different geometries for droplet trap-and-release, alternating distribution and path switching, based on droplet bistability. For all cases, the width of the main straight channel was $w = 200 \mu\text{m}$, that of the restrictions was $w_r = 30 \mu\text{m}$, and the height of the channel was $h = 50 \mu\text{m}$.

Flows of the dispersed phase (DI water) and the continuous phase (Silicone oil, 50 cS) can be precisely

controlled by two syringe pumps (Model 100, 210 series, kdScientific). Droplets were generated at the microchannel’s T-shaped junction. Frequency of the droplet generation and the length of the droplets can be modulated by controlling the flow rates of both the continuous phase and the dispersed phase. In our experimental flow conditions, the length of the droplet was always longer than the width of the main channel and the droplets did not wet the PDMS channel, while the continuous phase formed a thin liquid film layer between the droplet and the channel wall.

The Du Nouy ring method was adopted to measure the interfacial tension between DI water and silicone oil, which plays an important role in droplet bistability. Interfacial tension was measured at a constant temperature of 20°C by using a water bath with a temperature variation of less than 0.1°C and the data were averaged over five measurements.

The optical setup consisted of a halogen lamp, an epifluorescence microscope (IX50, Olympus) and a cooled-CCD camera (SensiCam, Cooke) and 4X and 10X objective lenses.

3 Results and discussions

3.1 Trap-and-release

In the droplet-based microfluidic systems, the droplet trap-and-release function is frequently required for monitoring chemical or biological assays at the designated location for a designated time (Schmitz et al. 2009; Huebner et al. 2009; Bai et al. 2010). The droplet trap-and-release function can be achieved by utilizing bistable geometry in the microfluidic devices. The droplet minimizes its surface energy which is defined as the product of interfacial tension and the surface area of the interface by adopting the smallest surface area. For a droplet of constant volume, surface energy is lowest when the droplet is spherical shaped. Surface energy then increases as the droplet is squeezed in a microchannel. When a droplet traveling in a straight channel encounters a narrow restriction, the droplet must deform its shape to pass through the restriction. Because a water droplet is non-wetting on the channel wall, the pressure difference across the droplet can be expressed by using the difference between the Laplace pressure at the restriction side and that at the channel side, and by representing the radii of curvature approximately with the widths of the restriction and the channel (Wang et al. 2009; Zagnoni and Cooper 2010):

$$(P_{in} - P_2) - (P_{in} - P_1) = 2\gamma\left(\frac{1}{w_r} + \frac{1}{h}\right) - 2\gamma\left(\frac{1}{w} + \frac{1}{h}\right) \tag{1}$$

where P_{in} , P_1 , and P_2 denote the pressure inside the droplet, the pressure outside of the droplet at the channel

side, and the pressure outside of the droplet at the restriction side, respectively. Therefore, the maximum pressure that a droplet can withstand without passing through the restriction can be expressed in the form of apparent Laplace pressure (the difference between the two Laplace pressures), as follows:

$$P_L = 2\gamma\left(\frac{1}{w_r} - \frac{1}{w}\right) \tag{2}$$

In the present experiments, $P_L \approx 2.6$ kPa for measured interfacial tension of $\gamma = 45.9$ mN/m. The bistable geometry is comprised of two symmetric branches with restrictions at the respective ends, as shown in Fig. 1. A droplet can pass through either of the restrictions in two different ways depending on a certain critical flow rate, where the total flow rate Q is expressed by the sum of the flow rates of the continuous phase (Q_c) and the dispersed phase (Q_d), under the constant flow rate condition. When a droplet enters the bifurcation channel, it flows into either the upper or lower branch and encounters a restriction, and then it is immediately trapped in front of the restriction and blocks the flow of the continuous phase into the restriction. Therefore, the continuous phase flows through the opposite branch of the bifurcation channel. In this situation, the trapped droplet can either stay in front of the restriction indefinitely or pass through it depending on the value of Q .

To simplify the problem, the hydrodynamic resistance model is introduced (Engl et al. 2005; Jousse et al. 2006; Cristobal et al. 2006). Then, the pressure difference across the droplet can be expressed by the pressure drop of the continuous phase, as follows:

$$\Delta P = P_1 - P_2 = QR \tag{3}$$

where R denotes the hydrodynamic resistance of the branch channel. If the pressure difference is lower than the apparent Laplace pressure (P_L), a droplet stays in front of the restriction indefinitely. Otherwise, that droplet passes through the restriction. By combining Eqs. 2 and 3, the critical flow rate can be expressed as follows:

$$Q^* = \frac{2\gamma}{R}\left(\frac{1}{w_r} - \frac{1}{w}\right) \tag{4}$$

Therefore, for the case when $Q > Q^*$, a droplet passes through the restriction regardless of the succeeding droplet, which results in a random choice of the path between the two branches. For the case when $Q < Q^*$, the droplet “A” in Fig. 1a is trapped until the next droplet “B” arrives at the opposite restriction. When droplet “B” blocks the opposite restriction, the upstream pressure increases instantaneously so that a momentary jump in $P_1 - P_2$ occurs surpassing P_L . Then the droplet “A,” which has already slightly deformed its surface shape at the restriction due to the operating pressure difference, $P_1 - P_2$ (which is

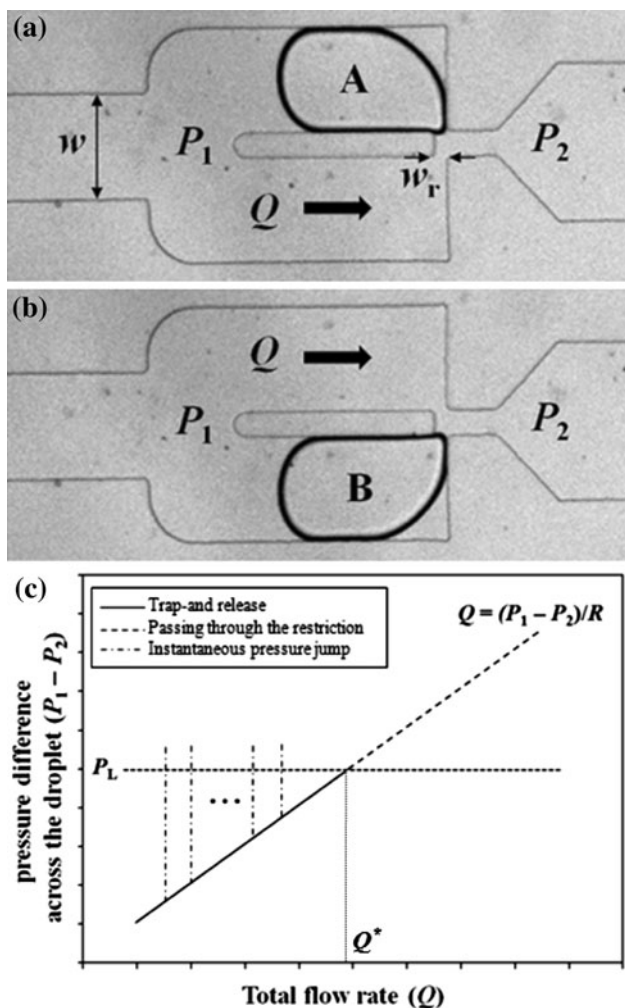


Fig. 1 Photomicrograph of the trap-and-release device with $w = 200 \mu\text{m}$ and $w_r = 30 \mu\text{m}$, and the relevant schematic. P_1 and P_2 denote the pressures about the trapped droplet, and Q denotes the total flow rate which is the sum of the flow rates of the dispersed phase (Q_d) and the continuous phase (Q_c). **a** A droplet is trapped at the upper branch and the continuous phase flows through the lower branch. **b** Another droplet is trapped at the lower branch and the continuous phase flows through the upper branch. **c** A schematic illustrating the relation of the total flow rate (Q) with the operating pressure difference across the droplet ($P_1 - P_2$) and the apparent Laplace pressure (P_L): trap-and-release is triggered regularly by an instantaneous jump in ($P_1 - P_2$) indicated as a vertical dash-dot line at a fixed total flow rate (Q)

lower than P_L), is released firstly so that the flow direction of the continuous phase is switched to the opposite channel, while droplet “B” is trapped as depicted in Fig. 1b. With the same hydrodynamic resistance R and the same flow rate Q , trap-and-release occurs repeatedly, which is triggered by the succeeding droplets in an alternating manner as shown in Fig. 2 (see Movie 1 in the Supplementary Material).

To investigate the flow condition for this droplet bistability, the flow rates of the water and oil phases were varied

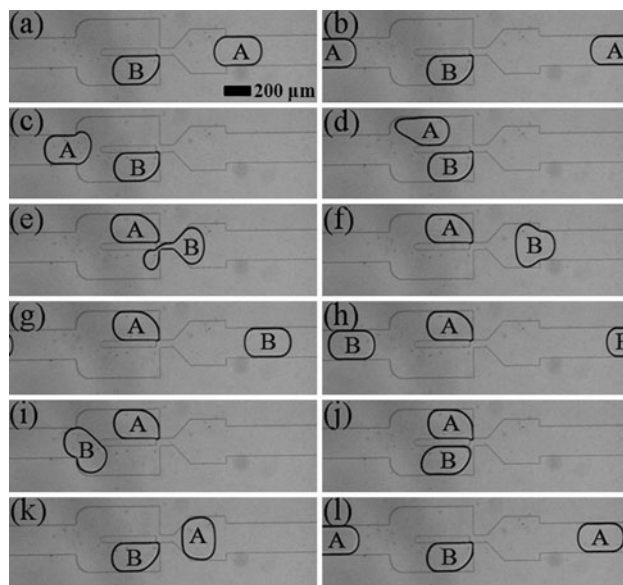


Fig. 2 Operation of droplet trap-and-release function triggered by succeeding droplets with $Q_d = 30 \mu\text{L/h}$ and $Q_c = 70 \mu\text{L/h}$. Droplets “A” and “B” travel through the upper and lower branches, respectively and repeatedly. Time interval between the images is 133 ms

in the ranges of 5–50 and 10–120 $\mu\text{L/h}$, respectively, so that the resulting droplet velocity and droplet length were in the ranges of 500–4200 $\mu\text{m/s}$ and 200–500 μm , respectively. Droplet velocity and droplet length were measured in the upstream straight channel far prior to the bifurcation channel to avoid the fluctuation of the droplet velocity which was induced from the pressure fluctuation when a droplet entered the bifurcation channel.

An assessment of the successful operation of trap-and-release function in the bistable geometry is provided in Fig. 3 in terms of droplet velocity versus droplet length. It essentially demonstrates that trap-and-release function in an alternating manner resulting from the droplet bistability

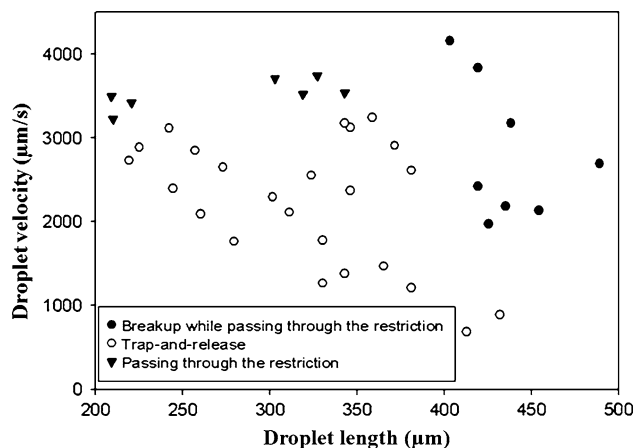


Fig. 3 Operation regime for trap-and-release function

is obtained in a certain range of parameters corresponding to the droplet velocity less than 3150 $\mu\text{m/s}$ which represents the critical velocity, and to the droplet length less than about 400 μm where droplet breakup resulting from Rayleigh-Plateau instability is prevented. Outside this range of parameters, a droplet either passed through the restriction by itself due to the high flow rate (i.e., $Q > Q^*$) or was broken and then partially merged with the other trapped droplet. Droplet breakup while passing through the restriction was the result of Rayleigh-Plateau instability, which was in good accordance with the tendency of droplet breakup at T-shaped junction (Link et al. 2004).

3.2 Droplet traffic control

There are increasing requirements for droplet traffic control at the interconnected junction, especially in the parallelized system for HTS. Most passive methods of droplet traffic control utilize the difference of hydrodynamic resistance resulting from the existence of droplets (Engl et al. 2005; Jousse et al. 2006; Cristobal et al. 2006; Cybulski and Garstecki 2010). However, recent studies have indicated the complexities of controlling droplet traffic at the interconnected junction because the hydrodynamic resistance of a branch depends on various parameters such as the number, size, and viscosity of the droplets contained therein (Jousse et al. 2006; Cybulski and Garstecki 2010). Although Cristobal et al. (2006) reported an efficient passive regulation method by introducing a microfluidic bypass to induce short-time memory, an alternating distribution function worked under very restricted flow conditions, which was mainly determined by the spacing between the droplets. To overcome the complexity and the limitation, we utilized droplet bistability for droplet traffic control such as alternating distribution of the droplets and droplet path switching.

3.2.1 Alternating distribution of droplets

Droplet bistability intrinsically distributes droplets in an alternating manner at the bifurcation channel for a trap-and-release function, which contains a single inlet channel and a single outlet channel. We modified the bistable geometry and the outlet channel in order to implement the alternating distribution of droplets. The modification proceeded in such a manner that the bistable geometry was connected with a single inlet channel and two outlet channels, which were separated by a micropillar array, as shown in Fig. 4.

The pressure difference across the droplet plays an important role in the droplet bistability, also as previously discussed. The bistable geometry for trap-and-release still displays the bistable mechanism because each branch

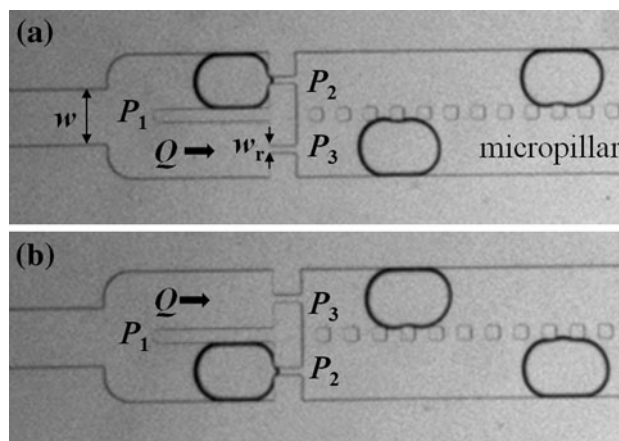


Fig. 4 Photomicrograph of the alternating distribution device, where the bifurcation channel has an inlet of $w = 200 \mu\text{m}$ and two restrictions of $w_r = 30 \mu\text{m}$, and the two outlet channels are separated by a micropillar array in between with $50 \mu\text{m}$ square pillars at intervals of $50 \mu\text{m}$. P_2 denotes the outlet pressure where a droplet blocks the continuous phase and P_3 denotes the outlet pressure where the continuous phase flows through the restriction. **a** A droplet is trapped at the upper branch and the continuous phase flows through the lower branch. **b** Another droplet is trapped at the lower branch and the continuous phase flows through the upper branch

shares the same inlet pressure, P_1 , and the same outlet pressure, P_2 , across the droplet, as demonstrated in the previous subsection. However, in the present case, two different outlet pressures exist at the two outlets, namely, P_2 and P_3 ($P_3 > P_2$). Therefore, the difference between P_2 and P_3 exists and modifies the operation range of the droplet bistability, so that a method must be devised to regulate P_2 and P_3 to effectively achieve droplet bistability. In the present section, a micro pillar array was inserted in the middle of the outlet chamber to divide it into two outlet channels, allowing the continuous phase to flow through the bypasses between the micro pillars. However, the dispersed phase (droplets) was effectively prevented from passing across the array. For the case when a droplet is trapped at the upper branch of the bifurcation channel, as Fig. 4a depicts, the continuous phase flows through the lower branch and through the restriction with the flow rate Q and $P_2 < P_3$. After passing through the restriction, one half of the continuous phase ($Q/2$) flows straight through the lower outlet channel, but the other half flows into the upper outlet channel through the bypasses, and vice versa until the downstream pressures of the two outlet channels become equalized. For bistability, the pressure difference across the droplet must be lower than the apparent Laplace pressure as expressed below:

$$P_1 - P_2 < P_L \tag{5}$$

The pressure drop associated with the flow of the continuous phase can be expressed as follows with the hydrodynamic resistance R' :

$$P_1 - P_3 = R'Q \quad (6)$$

Therefore, the difference between the two outlet pressures must satisfy the following relation for the droplet bistability:

$$P_3 - P_2 < P_L - R'Q \quad (7)$$

Because the geometry of the branches of the bifurcation channel is similar to the geometry of those used for trap-and-release, it can be assumed that $R' \sim R$. Then, the critical flow rate for alternating distribution, Q^{**} , can be expressed as follows:

$$Q^{**} = \frac{P_L}{R} - \frac{P_3 - P_2}{R} = Q^* - \frac{P_3 - P_2}{R} \quad (8)$$

From Eq. 8, it is expected that Q^{**} is lower than Q^* by the amount of $(P_3 - P_2)/R$.

A set of sequential photomicrographs showing a whole cycle of the alternating distribution of the droplets into the two outlet channels is given in Fig. 5. Remarkably, the droplets do not cross over the micropillar array because only the continuous phase is vented through the bypasses between adjacent micropillars. Therefore, once a droplet enters one of the two outlet channels, it flows downstream through that channel as far as the length of the micropillar array goes (see Movie 2 in the Supplementary Material). Figure 6 demonstrates that alternating distribution function resulting from droplet bistability is obtained under the critical droplet velocity of around $2400 \mu\text{m/s}$, which is about 23.8% lower than the critical velocity for trap-and-release, corresponding to $P_3 - P_2 = 619 \text{ Pa}$ (23.8% of P_L as can be estimated from Eq. 7). Except for the value of the critical velocity, the regime map for alternating distribution looks similar to that for the trap-and-release. Further, it

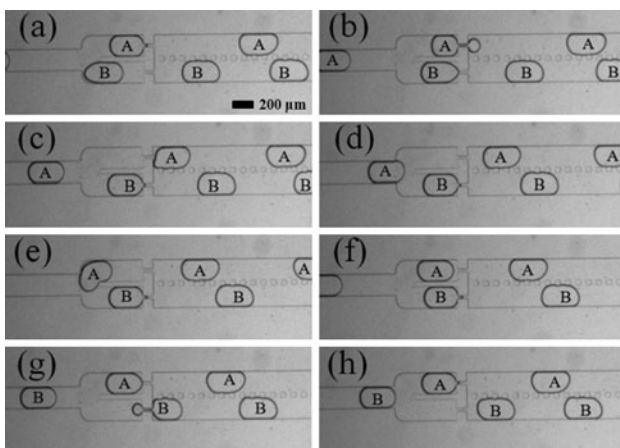


Fig. 5 Operation of alternating distribution of droplets, triggered by succeeding droplets with $Q_a = 20 \mu\text{L/h}$ and $Q_c = 50 \mu\text{L/h}$. Droplets “A” and “B” travel through the upper and lower branches and then are distributed to the upper and lower outlet channels, respectively. Time interval between the images is 133 ms

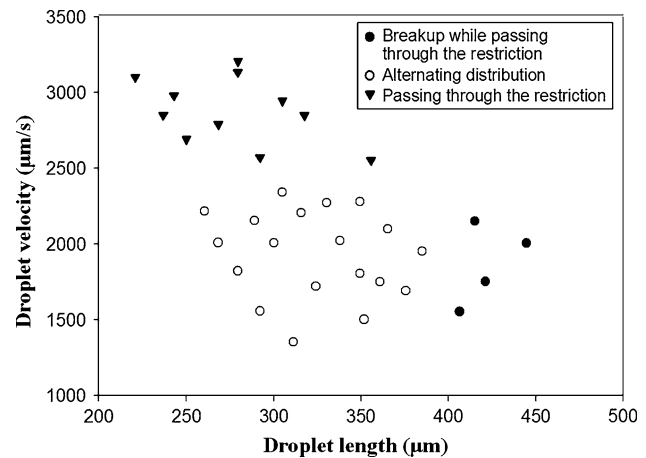


Fig. 6 Operation regime for alternating distribution function

should be remarked that the implementation of bistable geometry and the micropillar network can be useful for droplet synchronization and merging, as shown in Fig. 7. This discovery constitutes further research to supplement the present investigation.

3.2.2 Alternating path switching

In microfluidics, transporting droplets across another microchannel path is very difficult. This is as if the single-layer wiring is a very difficult problem in the design of printed circuit board. While the autonomous flow switching method that utilizes elastomeric components for a single phase fluid has been recently studied (Mosadegh et al. 2010), a study on the transport of the droplets across another microchannel path in a single-layer device without any external components does not yet exist.

Droplet path switching can be achieved by connecting the bistable geometry for the alternating distribution device with two outlet channels containing a single bypass between them, as shown in Fig. 8. In this device, the droplets’ paths are switched at the bifurcation junction

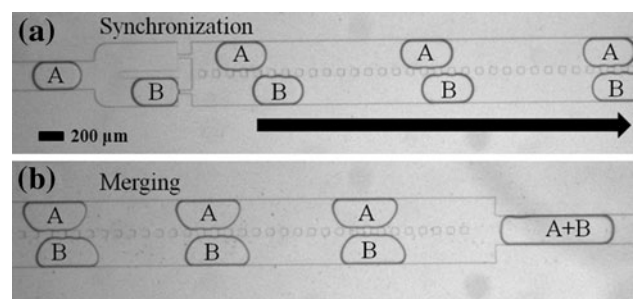


Fig. 7 **a** Multiple pairs of the droplets are synchronized while traveling through the two outlet channels separated by a micropillar array. **b** Synchronized pairs of droplets are merged at the end of the outlet channels

where the bypass is located. The difference in the shear forces, which is experienced by each droplet, determines the path of the droplet, directing it to the channel with high shear force (Tan et al. 2008). When the system is at a bistable state, the continuous phase flows with a flow rate Q into either the upper or the lower branch, and then it is divided into one of the two straight outlet channels and the bypass in between, with flow rates of Q_3 and Q_2 , respectively, as Fig. 8 depicts.

When the trapped droplet is released by the succeeding droplet, the released droplet encounters the bifurcation junction at which it experiences two different shear forces. The ratio of the shear force exerted on the droplet by the flow into the bypass to that by the flow into the straight channel depends on the flow rates (Q_2, Q_3) and the channel widths (w_b, w) (Tan et al. 2008). For any droplet, if the shear force ratio is greater than 1, the droplet switches its path to the bypass. Otherwise, the droplet should keep going straight without switching its path. From our observation, the ratio of the flow rate into the straight channel to that into the bypass, Q_2/Q_3 , was estimated around 0.8, which resulted in a shear force ratio of 14.88 with $w = 200 \mu\text{m}$ and $w_b = 50 \mu\text{m}$. Thus, the bistable

geometry in conjunction with a single bypass in between the two outlet channels led droplets to flow into the bypass even though the flow rate of the straight channel was higher than that of the bypass. As Fig. 9 shows, droplets switched through the bypass in an alternating manner, which was triggered by the succeeding droplets in a bistable state (see Movie 3 in the Supplementary Material). For bistability, the pressure difference across the droplet must be lower than the apparent Laplace pressure as expressed below:

$$P_1 - P_2 < P_L \tag{9}$$

Therefore, the critical flow rate Q^{***} for the alternating path switching can be expressed as follows:

$$Q^{***} = \frac{P_L}{R} - \frac{P_3 - P_2}{R} = Q^* - \frac{P_3 - P_2}{R} \tag{10}$$

The expression for Q^{***} takes the same form as for Q^{**} . However, a single bypass induces a larger outlet pressure difference, $P_3 - P_2$, than that for alternating distribution, which results in $Q^{***} < Q^{**}$.

Figure 10 demonstrates that path switching function, resulting from the droplet bistability, is obtained under a critical droplet velocity of $1500 \mu\text{m/s}$, which is lower than that for alternating distribution, as expected, with a maximum value of $P_3 - P_2 = 1362 \text{ Pa}$ (52.3% of P_L). Because a large difference in the outlet pressures significantly limits the range of operating flow rates for the droplet path switching, a careful design of the channel is required in order to reduce the outlet pressure difference. In particular,

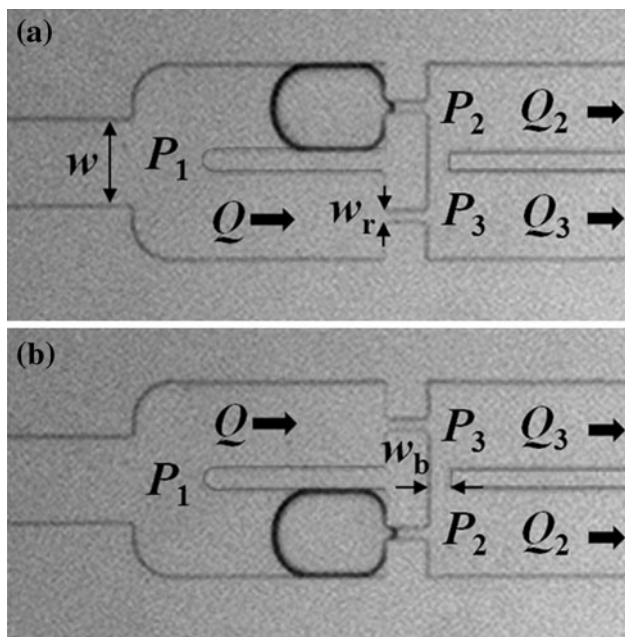


Fig. 8 Photomicrograph of the droplet path switching device which connects the bistable geometry for the alternating distribution device with two outlet channels which has a single bypass in between them, where $w_b = 50 \mu\text{m}$, $w = 200 \mu\text{m}$, and $w_r = 30 \mu\text{m}$. P_2 denotes the outlet pressure where a droplet blocks the continuous phase and P_3 denotes the outlet pressure where the continuous phase flows through the restriction. **a** A droplet is trapped at the upper branch and the continuous phase flows through the lower branch. **b** Another droplet is trapped at the lower branch and the continuous phase flows through the upper branch

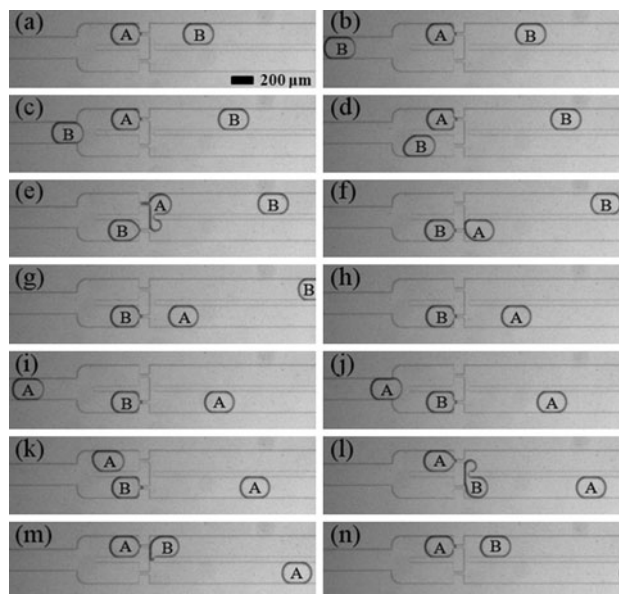


Fig. 9 Operation of droplet path switching, triggered by succeeding droplets with $Q_d = 5 \mu\text{L/h}$ and $Q_c = 50 \mu\text{L/h}$. Droplets “A” and “B” travel through the upper and lower branches and then are switched to the lower and upper outlet channels, respectively. Time interval between the images is 266 ms

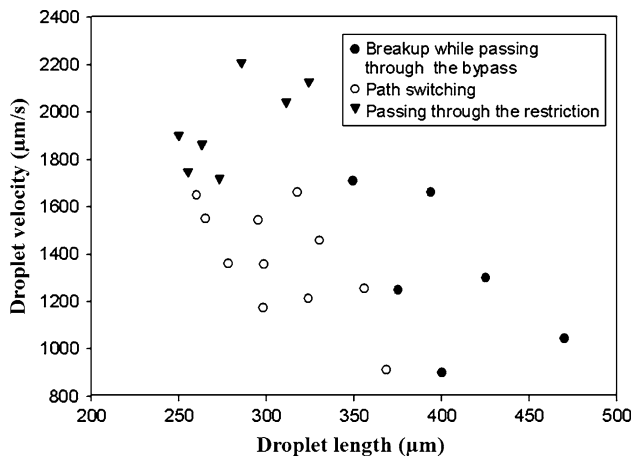


Fig. 10 Operation regime for path switching function

increasing the width of the bypass can lower the outlet pressure difference. However, it should be less than the width of the straight channel in order to satisfy the criterion for the alternating path switching, which requires that the shear force ratio is greater than unity. In our experiment, we did not observe the droplet path switching function for the case in which $w_b = 200 \mu\text{m}$ with $Q_2 \approx Q_3$. For the path switching geometry, droplet breakup occurred at the bypass while droplets passed through the bypass under the flow condition of smaller droplet length and velocity, in comparison with the flow conditions for droplet breakup at the restriction for trap-and-release and alternating distribution, as shown in Fig. 10.

4 Conclusion

We have demonstrated experimentally droplet bistability in microfluidic devices by implementing bistable geometry. Droplet bistability was achieved by repeatedly trapping and releasing droplets, which were triggered by the succeeding droplets in an alternating manner. The critical flow rate for achieving droplet bistability was attained, which was determined by the competition between the apparent Laplace pressure due to the interfacial tension and the pressure drop across the droplet due to the flow of the continuous phase. In other words, droplet bistability occurs when the ratio of the apparent Laplace pressure to the pressure drop across the droplet surpasses unity. By an appropriate channel design to induce droplet bistability, droplet traffic control was achieved at the bifurcation channel with a single inlet channel and two outlet channels. In particular, we distributed droplets at a junction in a manner of path alternation and path switching between the two outlet channels. A significant advantage of droplet bistability is that its operation is not affected by its

operating frequency below certain critical total flow rate, which makes our device robust with time-varying flow conditions while other passive methods often fail to operate precisely. The cost of fabrication, size of the device and the complexity of processing for droplet control can be reduced significantly by utilizing the droplet bistability. Moreover, bistable components can be easily integrated with other microfluidic components because bistable mechanism provides cascability. In an integrated fashion, they can be used as elaborately embedded droplet traffic signals for red light (trap), green light (release), and turn light (switching) in parallelized complex microfluidic devices. Finally, it is noteworthy that the control of the droplets was practically achieved by exploiting a microfluidic logic device. In contrast, most studies focused on establishing various logic gates but still lacked practical applicability, even though a microfluidic logic device has a great potential for manipulation of immiscible fluids.

Acknowledgments This research was supported by the Priority Research Program (2010-0029613) through the National Research Foundation of Korea (NRF) funded by the Ministry of Education, Science and Technology, Republic of Korea.

References

- Ahmed D, Mao X, Shi J, Juluri BK, Huang TJ (2009) A millisecond micromixer via single-bubble-based acoustic streaming. *Lab Chip* 9:2738–2741
- Bai Y, He X, Liu D, Patil SN, Bratton D, Huebner A, Hollfelder F, Abell C, Huck WTS (2010) A double droplet trap system for studying mass transport across a droplet–droplet interface. *Lab Chip* 10:1281–1285
- Chabert M, Viovy J-L (2008) Microfluidic high-throughput encapsulation and hydrodynamic self-sorting of single cells. *Proc Natl Acad Sci* 105:3191–3196
- Chabert M, Dorfman KD, Viovy J-L (2005) Droplet fusion by alternating current (AC) field electrocoalescence in microchannels. *Electrophoresis* 26:3706–3715
- Cheow LF, Yobas L, Kwong D-L (2007) Digital microfluidics: droplet based logic gates. *Appl Phys Lett* 90:054107
- Chokkalingam V, Weidenhof B, Krämer M, Maier WF, Herminghaus S, Seemann R (2010) Optimized droplet-based microfluidics scheme for sol–gel reactions. *Lab Chip* 10:1700–1705
- Cristobal G, Benoit J-P, Joanicot M, Ajdari A (2006) Microfluidic bypass for efficient passive regulation of droplet traffic at a junction. *Appl Phys Lett* 89:034104
- Cybulski O, Garstecki P (2010) Dynamic memory in a microfluidic system of droplets traveling through a simple network of microchannels. *Lab Chip* 10:484–493
- Engl W, Roche M, Colin A, Panizza P (2005) Droplet traffic at a simple junction at low capillary numbers. *Phys Rev Lett* 95:208304
- Franke T, Abate AR, Weitz DA, Wixforth A (2009) Surface acoustic wave (SAW) directed droplet flow in microfluidics for PDMS devices. *Lab Chip* 9:2625–2627
- Huebner A, Bratton D, Whyte G, Yang M, de Mello AJ, Abell C, Hollfelder F (2009) Static microdroplet arrays: a microfluidic

- device for droplet trapping, incubation and release for enzymatic and cell-based assays. *Lab Chip* 9:692–698
- Hung L-H, Choi KM, Tseng W-Y, Tan Y-C, Shea KJ, Lee AP (2006) Alternating droplet generation and controlled dynamic droplet fusion in microfluidic device for CdS nanoparticle synthesis. *Lap Chip* 6:174–178
- Jin B-J, Kim YW, Lee Y, Yoo JY (2010) Droplet merging in a straight microchannel using droplet size or viscosity difference. *J Micromech Microeng* 20:035003
- Jousse F, Farr R, Link DR, Fuerstman MJ, Garstecki P (2006) Bifurcation of droplet flows within capillaries. *Phys Rev E* 74:036311
- Lee C-H, Hsiung S-K, Lee G-B (2007) A tunable microflow focusing device utilizing controllable moving walls and its applications for formation of micro-droplets in liquids. *J Micromech Microeng* 17:1121–1129
- Lee C-Y, Lin Y-H, Lee G-B (2009) A droplet-based microfluidic system capable of droplet formation and manipulation. *Microfluid Nanofluid* 6:599–610
- Link DR, Anna SL, Weitz DA, Stone HA (2004) Geometrically mediated breakup of drops in microfluidic devices. *Phys Rev Lett* 92:054503
- Mosadegh B, Kuo C-H, Tung Y-C, Torisawa Y-s, Bersano-Begey T, Tavana H, Takayama S (2010) Integrated elastomeric components for autonomous regulation of sequential and oscillatory flow switching in microfluidic devices. *Nat Phys* 6:433–437
- Nisisako T, Torii T, Higuchi T (2002) Droplet formation in a microchannel network. *Lab Chip* 2:24–26
- Niu X, Gulati S, Edel JB, deMello AJ (2008) Pillar-induced droplet merging in microfluidic circuits. *Lab Chip* 8:1837–1841
- Prakash M, Gershenfeld N (2007) Microfluidic bubble logic. *Science* 315:832–835
- Schmitz CHJ, Rowat AC, Köster S, Weitz DA (2009) Dropspots: a picoliter array in a microfluidic device. *Lab Chip* 9:44–49
- Shim J-u, Cristobal G, Link DR, Thorsen T, Jia Y, Piattelli K, Fraden S (2007) Control and measurement of the phase behavior of aqueous solutions using microfluidics. *J Am Chem Soc* 129:8825–8835
- Shintaku H, Kuwabara T, Kawano S, Suzuki T, Kanno I, Kotera H (2007) Micro cell encapsulation and its hydrogel-beads production using microfluidic device. *Microsyst Technol* 13:951–958
- Tan Y-C, Fisher JS, Lee AI, Cristini V, Lee AP (2004) Design of microfluidic channel geometries for the control of droplet volume, chemical concentration, and sorting. *Lab Chip* 4:292–298
- Tan Y-C, Ho YL, Lee AP (2007) Droplet coalescence by geometrically mediated flow in microfluidic channels. *Microfluid Nanofluid* 3:495–499
- Tan Y-C, Ho YL, Lee AP (2008) Microfluidic sorting of droplets by size. *Microfluid Nanofluid* 4:343–348
- Thorsen T, Roberts RW, Arnold FH, Quake SR (2001) Dynamic pattern formation in a vesicle-generating microfluidic device. *Phys Rev Lett* 86:4163–4166
- Toepke MW, Abhyankar VV, Beebe DJ (2007) Microfluidic logic gates and timers. *Lap Chip* 7:1449–1453
- Wang W, Yang C, Li CM (2009) On-demand microfluidic droplet trapping and fusion for on-chip static droplet assays. *Lab Chip* 9:1504–1506
- Xia Y, Whitesides GM (1998) Soft lithography. *Annu Rev Mater Sci* 28:153–184
- Zagnoni M, Cooper JM (2010) A microdroplet-based shift register. *Lab chip* 10:3069–3073